PROCEEDINGS OF SCIENCE

# Study of downward Terrestrial Gamma-ray Flashes with the surface detector of the Pierre Auger Observatory

**Roberta Colalillo**[*,a,b] **for the Pierre Auger Collaboration**[c] **and Joseph Dwyer**[d]

[a] *Università degli Studi di Napoli "Federico II", Dipartimento di Fisica "E. Pancini", Via Cintia, 80126 Napoli, Italy*

[b] *INFN, Sezione di Napoli, Via Cintia, 80126 Napoli, Italy*

[c] *Observatorio Pierre Auger, Av. San Martín Norte 304, 5613 Malargüe, Argentina*
*Full author list:* https://www.auger.org/archive/authors_icrc_2023.html

[d] *University of New Hampshire, Department of Physics and Space Science Center (EOS), 8 College Road, 03824 Durham, NH, USA*

*E-mail:* spokespersons@auger.org

The surface detector (SD) of the Pierre Auger Observatory, consisting of 1660 water-Cherenkov detectors (WCDs), covers 3000 km$^2$ in the Argentinian pampa. Thanks to the high efficiency of WCDs in detecting gamma rays, it represents a unique instrument for studying downward Terrestrial Gamma-ray Flashes (TGFs) over a large area. Peculiar events, likely related to downward TGFs, were detected at the Auger Observatory. Their experimental signature and time evolution are very different from those of a shower produced by an ultrahigh-energy cosmic ray. They happen in coincidence with low thunderclouds and lightning, and their large deposited energy at the ground is compatible with that of a standard downward TGF with the source a few kilometers above the ground. A new trigger algorithm to increase the TGF-like event statistics was installed in the whole array. The study of the performance of the new trigger system during the lightning season is ongoing and will provide a handle to develop improved algorithms to implement in the Auger upgraded electronic boards. The available data sample, even if small, can give important clues about the TGF production models, in particular, the shape of WCD signals. Moreover, the SD allows us to observe more than one point in the TGF beam, providing information on the emission angle.

38th International Cosmic Ray Conference (ICRC2023)
26 July – 3 August, 2023
Nagoya, Japan





PoS(ICRC2023)439

## 1. The Pierre Auger Observatory and the atmospheric electricity

The fluorescence and surface detector of the Pierre Auger Observatory [1], designed to study extensive air showers produced by the most energetic cosmic rays as they pass through the atmosphere, have a great potential for the detection of ELVES (Emission of Light and Very Low Frequency perturbations due to Electromagnetic Pulse Sources) and halos [2] and downward Terrestrial Gamma-ray Flashes (TGFs), which are bright events produced by lightning.

TGFs are millisecond bursts of gamma-rays originating from within the Earth's atmosphere during thunderstorms [3]. TGFs were firstly observed by BATSE in 1994 [4], and since then have been reported by many other satellites. Recently, the observation of downward TGFs and our knowledge about them have been increasing [5, 6]. The Pierre Auger Observatory surface detector (SD), consisting of 1600 Water Cherenkov Detectors (WCDs), has observed peculiar events during thunderstorms [7], now associated with downward TGFs [8, 9]. When charged particles, in particular electrons and muons, cross the SD station with speed greater than the speed of light in water, Cherenkov light is produced and collected by three PMTs looking into the water from the top. The height of 1.2 m makes WCDs also very sensitive to high energy photons, which convert to electron–positron pairs in the water volume. A "standard" upward TGF produces about $10^{17}$ gamma rays of energy from 1 to 20 MeV in the primary beam. Therefore, WCDs, with a threshold for gammas of few MeV, are perfect instruments for their detection. Downward TGFs have an experimental signature and a time evolution very different from those of a shower produced by an ultrahigh-energy cosmic ray. The multiplicity of triggered SD stations is much larger than that due to extensive air showers, the footprint covers about 200 km$^2$, as shown in figure 1, and the signals observed in the WCDs last more than 10 $\mu$s, one order of magnitude longer than the duration of the signal produced by cosmic-ray showers.

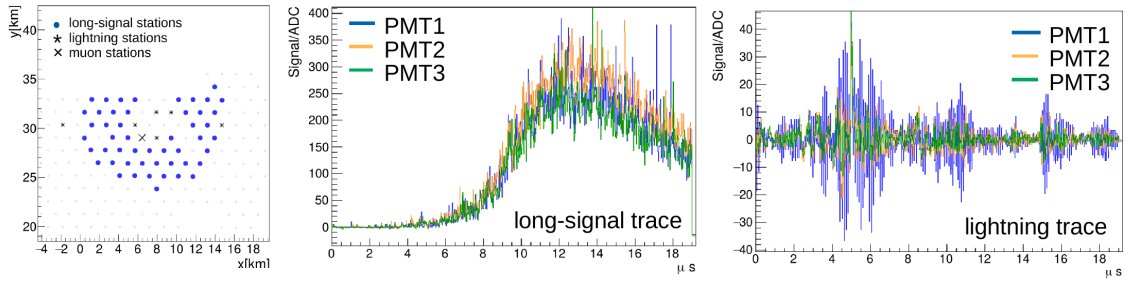


**Figure 1:** Left: the large footprint of a TGF event. Long-signal stations are marked in blue, lightning stations with stars, and muon stations with crosses. Center: a long signal read by the three PMTs which are in each Water-Cherenkov detector. Right: a lightning signal due to high-frequency noise. The presence of at least a lighting station in each event suggested that they happened during thunderstorms.

The TGF radiation hits the central stations first and reaches the external ones in tens of microseconds. A single event can activate two or more consecutive triggers. Moreover, during thunderstorms, the trigger rate massively increases. All these deviations from cosmic-ray shower behaviour suggested that the low statistics of Auger downward TGFs (less than 2 events/year, while at least 30 events/year are expected) and the lack of signals in the center of the footprint have not a physical origin but are due to electronics, trigger, data acquisition, or post-acquisition processing



PoS(ICRC2023)439

of the Auger SD optimized for rate, shape and signals of cosmic-ray showers. This hypothesis was verified as described in [8] and an ad-hoc trigger algorithm to identify TGFs was designed and implemented in the electronic board of each WCD since November 2021 [10] without compromising normal data taking. In the meantime, the installation of the new electronic boards for AugerPrime [11], the Pierre Auger Observatory upgrade, has begun, and new work is now required to optimise the surface detector for TGF studies exploiting the potential of new electronics and detectors and the experience gained with the previous configuration.

In this proceeding, the data collected so far are analysed to increase the knowledge about downward TGFs and constrain models on their production mechanisms.

## 2. Downward TGFs and production mechanisms

TGF photons are produced via the bremsstrahlung process when a cascade of energetic electrons forms in coincidence with lightning. It has been debated so far which exact mechanism in lightning discharges is responsible for the acceleration of electrons to relativistic energies. In fact, only if electrons reach energies larger than approximately 150–200 eV, travelling in a thundercloud region that contains a strong electric field, they can gain enough energy to compensate the ionization loss and "runs away", activating the electron avalanches. For a long time, the "seed" electrons were thought to be remnants of cosmic-ray showers, but the recent measurements done by the ASIM experiment disfavour this idea [12], and two other models are now under debate. According to the "Lightning Leader" model [12], low-energy electrons are accelerated in the high-field regions localized in the vicinity of lightning leader tips, while the "Relativistic Feedback" model [13, 14] assumes that backscattered positrons and photons produced during the development of the electron avalanche can propagate to the start of the avalanche region and can produce additional runaway electrons. The number of runaway electron avalanches increases exponentially on a timescale of few microseconds. The available Auger data sample of downward TGFs can give important hints to distinguish between these two TGF production models and can also help to understand if there are differences between upward and downward TGFs. Moreover, thanks to the large number of SD stations, very sensitive to photons, we can study the spatial and temporal development of the TGF emission in detail. For upward TGFs, we expect gammas emitted within a cone with an angle of about 30°. From the first studies carried out, it was seen that the footprint at the ground produced by a similar emission propagating in the opposite direction is too small. The deposited energy per $m^2$ of an Auger TGF as a function of the distance from the center of the footprint is compatible with the expectation for a standard downward TGF with an isotropic emission into the lower hemisphere and the source at 1 and 2 km above the ground [9]. This height is compatible with the source height obtained fitting the signal arrival time in the Auger detectors assuming a spherical propagation [7].

## 3. Auger signals and the Relativistic Feedback Model

As explained in the previous section, the relativistic feedback mechanism predicts an exponential runaway electron flux at the source, the zone where the avalanche starts. TGF photons are produced via bremsstrahlung and then propagate through the atmosphere to reach the ground where they are detected. Reasonably, the photon production and their propagation do not strongly change

the time evolution, and we expect that also the arrival time of the photons in WCDs can be described by an exponential function.
In figure 2, some "long signals" typical of Auger TGF events are shown. Assuming that energetic

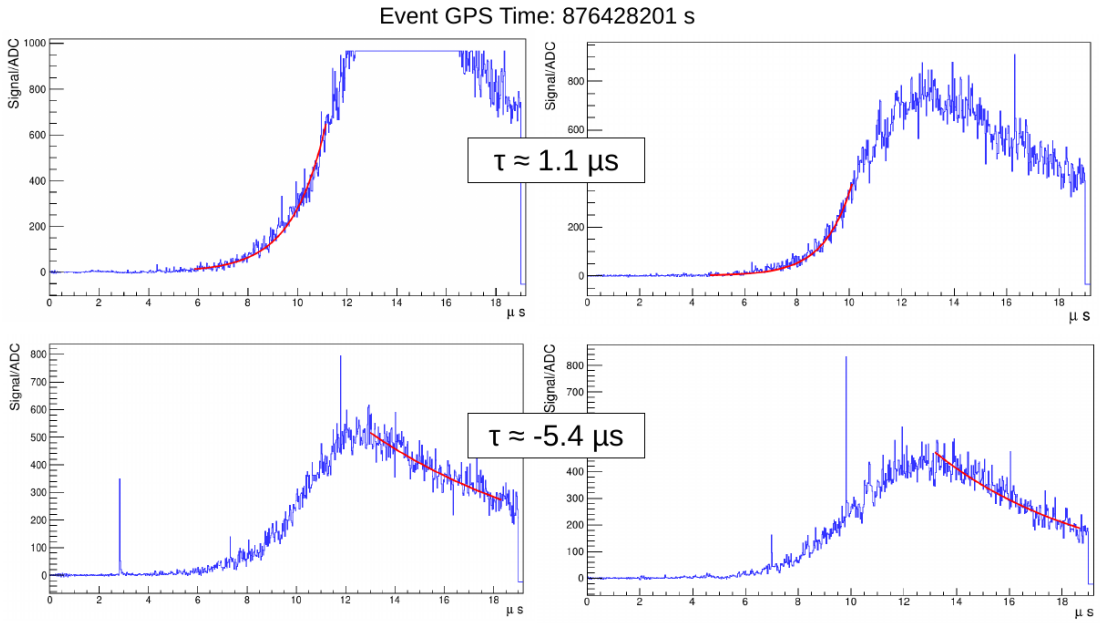


**Figure 2:** The rising and falling edge of the Auger long signals produced by a downward TGF are described by an exponential function as predicted by the relativistic feedback mechanism.

electrons are produced by the relativistic feedback mechanism, we foresee that the rising and falling edge of long signals follow an exponential evolution. In the top panel of figure 2, we can see that the rising edge of two long signals belonging to the same event are described by the same exponential function, $f(t) = exp(k + t/\tau)$, with $\tau \approx 1.1\ \mu$s. This is true for each signal of the event, while the $\tau$ value changes if we analyze a different event (see the signal in figure 3 belonging to a different event). Each TGF has, in fact, a peculiar evolution, and this is probably related to the characteristics of the thunderstorm that generated the TGF.
As it is evident observing the right plot in the upper panel of figure 2, only a part of the rising edge can be described by the exponential function. Before reaching the maximum, the slope of the signal changes. In figure 3, we divided the rising edge into two parts:

1. The red part, the exponential part, corresponds to the initial phase of the electron avalanche development. The runaway electron flux is low and the intense thundercloud electric field is not modified by the discharge current generated by the runaway electrons.

2. In the green part, the slope of the signal is changed, the runaway electron flux has grown enough that the current is able to counteract the thunderstorm field, and the avalanche generation starts slowing down and eventually stops.

In the falling edge, the runaway electron flux decreases, and the photon flux falls down exponentially. The decrease of the signal is slower than the increase, and in fact, in the event we are considering,

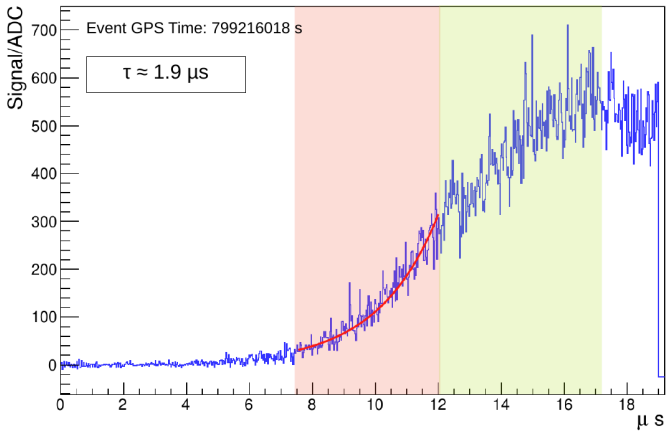


**Figure 3:** In the rising edge of the signal, after the first exponential part, a change in the signal evolution is evident. It is a hint of the growth of the runaway electron avalanche, which reaches such an intensity that the current produced by it counteracts the electric field of the thundercloud.
As expected, the exponential function describing this signal has a different $\tau$ respect to the signals shown in 2 belonging to another event.

the exponential has a tau approximately equal to -5.4 $\mu$s.
In our data sample, there are events very close in time (tens of minutes). They are probably produced by the same thunderstorm, and we expect similar characteristics. Their signals are described by exponential functions with the same $\tau$ value. Further investigation on this aspect are in progress.

## 4. TGF producing-storms: meteorological studies

All the upward TGF observations, associated mainly with intracloud lightning, have been correlated with regions of intense lightning, and it has been estimated that the source regions are at the altitudes of thunderstorm tops, typically 10–15 km above ground level. Instead, in the last years, evidence of downward TGFs, occurring during strong initial breakdown pulses in the first few milliseconds of negative cloud-to-ground and low-altitude intra-cloud flashes, has been reported [5, 6]. Thanks to the instruments for atmospheric monitoring available at the Pierre Auger Observatory, we verified that at the time of some downward TGFs, there were clouds with a very low base and with a large vertical development (see figure 4). Unfortunately, in Auger, most atmospheric monitoring devices are operated when the fluorescence detector is taking data, and, in most cases, are turned off when a thunderstorm is above the array. Therefore, our information is incomplete. Comparing our available data with the data provided each hour by the station of the Argentinian "Servicio Meteorológico Nacional" in Malargüe, we found a good agreement. A high cloud coverage was confirmed together with the presence of clouds with a low base height (1000/1500 m). In addition, also details about the cloud type are avalaible. For the event shown in figure 4, cumulonimbus was observed. Their upper part is fibrous (cirriform) and anvil-shaped. These are the typical characteristics of thunderstorm clouds.
In the previous section, we discussed the opened questions about the TGF production mechanisms, but also the knowledge about the TGF producing-storm is poor. An important point for understand-

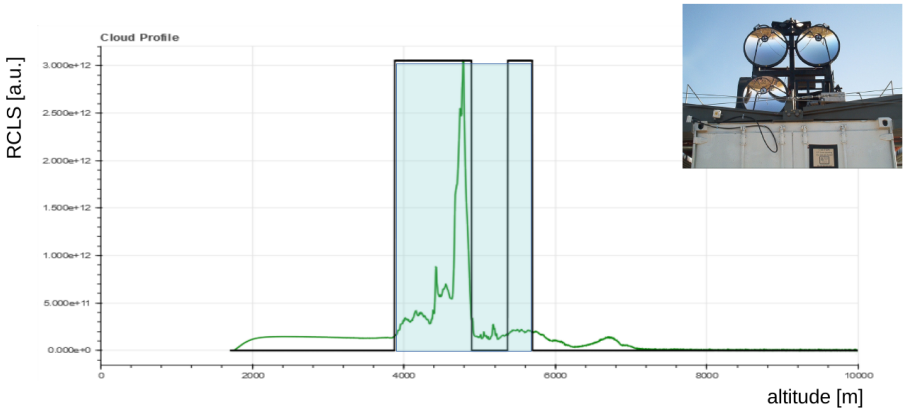


**Figure 4:** Lidar measurement (range-corrected lidar signal vs altitude above sea level) [15] showing a cloud with the base at about 2500 m above the Auger Observatory level, which develops vertically for about 2 km. The measurement was taken 54 minutes before the TGF event.

ing the TGF origin is to know in which phase of a thunderstorm the TGF starts and, in particular, at what stage in lightning development. Moreover, it is known that TGFs are produced by storms of all shapes and sizes, but it is still unknown why some thunderstorms produce TGFs, and others do not. It is possible that characteristics of thunderstorms themselves, such as seasonal conditions or ground altitude, electric field intensity, and atmospheric conditions, make intrinsic differences in the occurrence, brightness, and production mechanisms of downward TGFs. Last but not least, present knowledge is for upward TGFs [16], and it is possible that thunderstorm characteristics for downward TGFs are different as already verified for the cloud altitude. For these reasons, we started to analyze the meteorological conditions at the time of Auger TGF events. Most of them were collected before 2013, when a change in SD trigger conditions reduced our detection efficiency. Public available databases from satellite and land instruments were not as comprehensive as today, and we have to base on models to reproduce the weather conditions: therefore we use the ERA5 data. ERA5 is the fifth-generation ECMWF (European Centre for Medium-Range Weather Forecasts) atmospheric reanalysis of the global climate covering the period from January 1940 to the present. ERA5 provides hourly estimates of a large number of atmospheric, land, and oceanic climate variables. The data cover the Earth on a 30 km grid and resolve the atmosphere using 137 levels from the surface up to a height of 80 km.

So far, we analyzed two variables, the Convective Available Potential Energy (CAPE) and the Precipitable Water Vapor (PWV), which are shown in figure 5 for the 25$^{th}$ of December 2007. CAPE is the amount of energy available to a developing thunderstorm. More specifically, it describes the instability of the atmosphere and provides an approximation of updraft strength within a thunderstorm. A higher value of CAPE means the atmosphere is more unstable and would, therefore, produce a stronger updraft. At the same time, PWV is related to the total atmospheric water vapor contained in a vertical column of unit cross-sectional area extending between the Earth's surface and the "top" of the atmosphere. The amount of water in the atmosphere is an important factor that can, along with other factors, determine the amount of rainfall and influence the dynamical evolution of convective storms. When large amounts of PWV are observed, there is a greater probability of

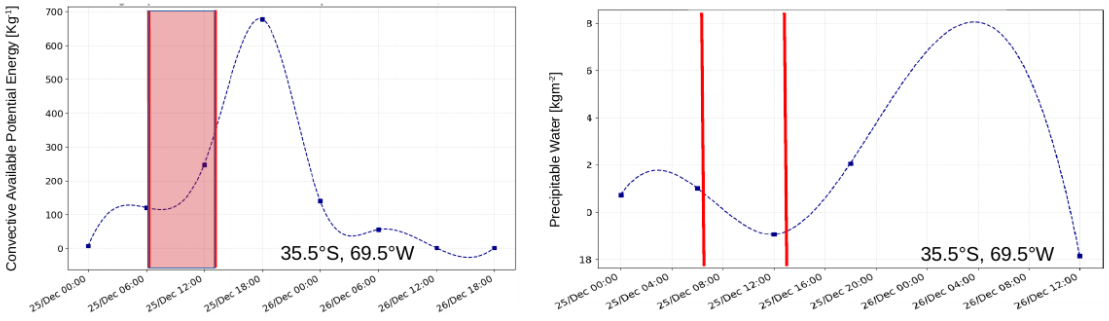


**Figure 5:** Convective Available Potential Energy (CAPE) -left- and Precipitable Water Vapor (PWV) -right- at the Pierre Auger Observatory latitude and longitude for the 25$^{th}$ of December 2007. The time of the six TGF events detected that day falls in the red band.

uplifting convection and cloud formation.
On the 25$^{th}$ of December 2007, six TGF events were detected. The red band in figure 5 represents the time interval in which the events occurred and is in the growth stage of CAPE and PWV. Also for other events, we observed they were detected in the growth stage of the two variables. This means that downward TGF events detected at the Pierre Auger Observatory occurred in the first phase of the storm. Obviously, we cannot exclude that other TGFs were produced during later stages of the thunderstorm evolution, but the acquisition system of the Auger SD, optimized for cosmic rays, may have prevented their recording.
In 2010, two E-field mills were installed at the Pierre Auger Observatory to measure the electric field strength at ground level, and provide auxiliary information for AERA (Auger Engineering Radio Array). AERA [17] can detect air showers studying the radio pulses in the MHz range emitted during the propagation of the shower front through the atmosphere. The strength of the emitted signal is highly influenced by large electric fields, in particular, amplified signals up to an order of magnitude have been detected as an effect of thunderstorms. In fact, the intense electric fields in thunderclouds induce strong electric fields at the ground, and the E-field mill signal can give a hint about the evolution of the thunderstorm. We have E-field measurements only in coincidence with a few TGF events. In figure 6, we can see the potential gradient measured by one of the two E-field mills the 6$^{th}$ of February 2013. The red line is the time of a TGF event, and, also in this case, we can see that the event occurs at the beginning of the thunderstorm. We showed the signal of the E-field mill closest to the event, but new E-mills have now been installed at the Observatory since radio antennas will be added to each WCD [11], so more punctual measurements will be possible in the future.

## Conclusion

Auger TGF events allow us to increase the knowledge about downward TGFs. The signals of these events are compatible with the expectations of the relativistic feedback mechanism, one of the two models that explain the TGF origin. Moreover, we verified that the deposited energy at the ground of the Auger TGF events is compatible with the one of a standard TGFs with an isotropic emission into the lower hemisphere and the source at 1 and 2 km above the ground. Further

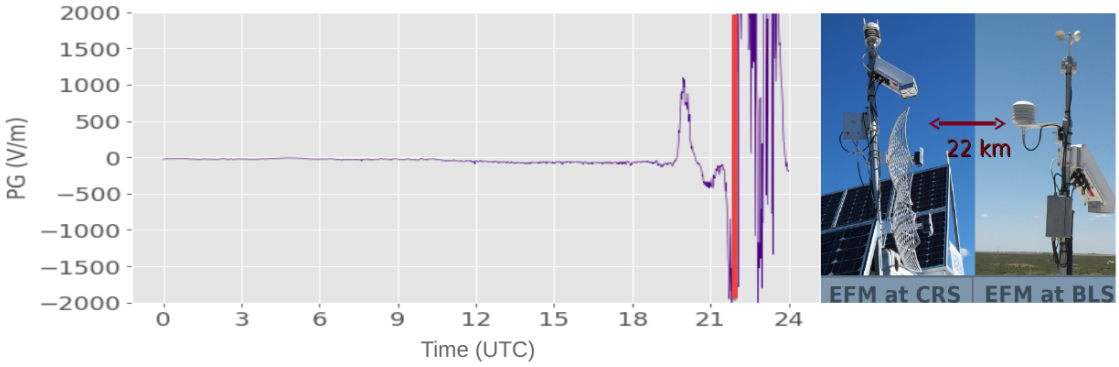


**Figure 6:** Left: potential gradient variations measured by one of the two E-field mills installed at the Pierre Auger Observatory. A TGF event, indicated by the red line, occurs at the beginning of the thunderstorm. Right: The two Campbell Scientific CS110 E-field mills installed at the Observatory.

studies are in progress to better understand the geometrical characteristics of gamma emission. The extension of the Observatory and the high sensitivity of the WCDs to gammas are very important to achieve this goal. Finally, we confirmed, thanks to the information provided by the station of the Argentinian "Servicio Meteorológico Nacional" in Malargüe, that the Auger downward TGFs occur in the presence of cumulonimbus with anvil, the typical thunderstorm clouds, and that the base of these clouds is very low. Studying CAPE and PWV in coincidence with Auger events, we observed that they occur at the beginning of a thunderstorm. Other variables are being investigated to understand the characteristics of the storms that cause TGFs.
AugerPrime will give new opportunities for the detection of downward TGFs, and we are working to improve the capabilities of the surface detector during lightning periods.

## References

[1] A. Aab *et al.*, Nucl. Instrum. Meth. A **798** (2015) 172–213.
[2] R. Mussa [for the Pierre Auger Coll.], these proceedings.
[3] J.R. Dwyer, D.M. Smith, and S.A. Cummer, Space Sci. Rev. **173** (2012) 133–196.
[4] G. J. Fishman et al., Science **264** (1994) 5163, 1313–1316.
[5] J.W. Belz et al. [Telescope Array Coll.], J. Geophys. Res. Atmos. **125** (2020) e2019JD031940.
[6] Y. Wada et al., Phys. Commun. **2** (2019) 67.
[7] R. Colalillo [for the Pierre Auger Coll.], Proc. 35th Int. Cosmic Ray Conf., Busan, Korea (2017), PoS(ICRC2017)314
[8] R. Colalillo [for the Pierre Auger Coll.], Proc. 37th Int. Cosmic Ray Conf., Berlin, Germany (2021), PoS(ICRC2021)395.
[9] R. Colalillo [for the Pierre Auger Coll.], EPJ Web of Conferences **283** (2023) 06014.
[10] M. Schimassek [for the Pierre Auger Coll.], J. Phys. Conf. Ser. **2398** (2022) 012003.
[11] A. Castellina for the Pierre Auger Collaboration, EPJ Web of Conferences **210** (2019) 06002.
[12] C. Köhn et al., Geophys. Res. Lett. **47** (2020) e2020GL089749.
[13] J. R. Dwyer, J. Geophys. Res. Space Physics **117** (2012) A02308.
[14] E. Stadnichuk et al., Atmos. Res. **277** (2022) 106329.
[15] J. Pallotta, J. Rodriguez [for the Pierre Auger Coll.], these proceedings.
[16] A. Tiberia et al., Rendiconti Lincei. Scienze Fisiche e Naturali **30** (2019) Suppl 1: S259-S263.
[17] A. Aab et al. (The Pierre Auger Collaboration), JINST **7** (2012) P10011.

## The Pierre Auger Collaboration

A. Abdul Halim[13], P. Abreu[72], M. Aglietta[54,52], I. Allekotte[1], K. Almeida Cheminant[70], A. Almela[7,12], R. Aloisio[45,46], J. Alvarez-Muñiz[79], J. Ammerman Yebra[79], G.A. Anastasi[54,52], L. Anchordoqui[86], B. Andrada[7], S. Andringa[72], C. Aramo[50], P.R. Araújo Ferreira[42], E. Arnone[63,52], J. C. Arteaga Velázquez[67], H. Asorey[7], P. Assis[72], G. Avila[11], E. Avocone[57,46], A.M. Badescu[75], A. Bakalova[32], A. Balaceanu[73], F. Barbato[45,46], A. Bartz Mocellin[85], J.A. Bellido[13,69], C. Berat[36], M.E. Bertaina[63,52], G. Bhatta[70], M. Bianciotto[63,52], P.L. Biermann[h], V. Binet[5], K. Bismark[39,7], T. Bister[80,81], J. Biteau[37], J. Blazek[32], C. Bleve[36], J. Blümer[41], M. Boháčová[32], D. Boncioli[57,46], C. Bonifazi[8,26], L. Bonneau Arbeletche[21], N. Borodai[70], J. Brack[j], P.G. Brichetto Orchera[7], F.L. Briechle[42], A. Bueno[78], S. Buitink[15], M. Buscemi[47,61], M. Büsken[39,7], A. Bwembya[80,81], K.S. Caballero-Mora[66], S. Cabana-Freire[79], L. Caccianiga[59,49], I. Caracas[38], R. Caruso[58,47], A. Castellina[54,52], F. Catalani[18], G. Cataldi[48], L. Cazon[79], M. Cerda[10], A. Cermenati[45,46], J.A. Chinellato[21], J. Chudoba[32], L. Chytka[33], R.W. Clay[13], A.C. Cobos Cerutti[6], R. Colalillo[60,50], A. Coleman[90], M.R. Coluccia[48], R. Conceição[72], A. Condorelli[37], G. Consolati[49,55], M. Conte[56,48], F. Convenga[41], D. Correia dos Santos[28], P.J. Costa[72], C.E. Covault[84], M. Cristinziani[44], C.S. Cruz Sanchez[3], S. Dasso[4,2], K. Daumiller[41], B.R. Dawson[13], R.M. de Almeida[28], J. de Jesús[7,41], S.J. de Jong[80,81], J.R.T. de Mello Neto[26,27], I. De Mitri[45,46], J. de Oliveira[17], D. de Oliveira Franco[21], F. de Palma[56,48], V. de Souza[19], E. De Vito[56,48], A. Del Popolo[58,47], O. Deligny[34], N. Denner[32], L. Deval[41,7], A. di Matteo[52], M. Dobre[73], C. Dobrigkeit[21], J.C. D'Olivo[68], L.M. Domingues Mendes[72], J.C. dos Anjos, R.C. dos Anjos[25], J. Ebr[32], F. Ellwanger[41], M. Emam[80,81], R. Engel[39,41], I. Epicoco[56,48], M. Erdmann[42], A. Etchegoyen[7,12], C. Evoli[45,46], H. Falcke[80,82,81], J. Farmer[89], G. Farrar[88], A.C. Fauth[21], N. Fazzini[e], F. Feldbusch[40], F. Fenu[41,d], A. Fernandes[72], B. Fick[87], J.M. Figueira[7], A. Filipčič[77,76], T. Fitoussi[41], B. Flaggs[90], T. Fodran[80], T. Fujii[89,f], A. Fuster[7,12], C. Galea[80], C. Galelli[59,49], B. García[6], C. Gaudu[38], H. Gemmeke[40], F. Gesualdi[7,41], A. Gherghel-Lascu[73], P.L. Ghia[34], U. Giaccari[48], M. Giammarchi[49], J. Glombitza[42,g], F. Gobbi[10], F. Gollan[7], G. Golup[1], M. Gómez Berisso[1], P.F. Gómez Vitale[11], J.P. Gongora[11], J.M. González[1], N. González[7], I. Goos[1], D. Góra[70], A. Gorgi[54,52], M. Gottowik[79], T.D. Grubb[13], F. Guarino[60,50], G.P. Guedes[22], E. Guido[44], S. Hahn[39], P. Hamal[32], M.R. Hampel[7], P. Hansen[3], D. Harari[1], V.M. Harvey[13], A. Haungs[41], T. Hebbeker[42], C. Hojvat[e], J.R. Hörandel[80,81], P. Horvath[33], M. Hrabovský[33], T. Huege[41,15], A. Insolia[58,47], P.G. Isar[74], P. Janecek[32], J.A. Johnsen[85], J. Jurysek[32], A. Kääpä[38], K.H. Kampert[38], B. Keilhauer[41], A. Khakurdikar[80], V.V. Kizakke Covilakam[7,41], H.O. Klages[41], M. Kleifges[40], F. Knapp[39], N. Kunka[40], B.L. Lago[16], N. Langner[42], M.A. Leigui de Oliveira[24], Y Lema-Capeans[79], V. Lenok[39], A. Letessier-Selvon[35], I. Lhenry-Yvon[34], D. Lo Presti[58,47], L. Lopes[72], L. Lu[91], Q. Luce[39], J.P. Lundquist[76], A. Machado Payeras[21], M. Majercakova[32], D. Mandat[32], B.C. Manning[13], P. Mantsch[e], S. Marafico[34], F.M. Mariani[59,49], A.G. Mariazzi[3], I.C. Mariş[14], G. Marsella[61,47], D. Martello[56,48], S. Martinelli[41,7], O. Martínez Bravo[64], M.A. Martins[79], M. Mastrodicasa[57,46], H.J. Mathes[41], J. Matthews[a], G. Matthiae[62,51], E. Mayotte[85,38], S. Mayotte[85], P.O. Mazur[e], G. Medina-Tanco[68], J. Meinert[38], D. Melo[7], A. Menshikov[40], C. Merx[41], S. Michal[33], M.I. Micheletti[5], L. Miramonti[59,49], S. Mollerach[1], F. Montanet[36], L. Morejon[38], C. Morello[54,52], A.L. Müller[32], K. Mulrey[80,81], R. Mussa[52], M. Muzio[88], W.M. Namasaka[38], S. Negi[32], L. Nellen[68], K. Nguyen[87], G. Nicora[9], M. Niculescu-Oglinzanu[73], M. Niechciol[44], D. Nitz[87], D. Nosek[31], V. Novotny[31], L. Nožka[33], A Nucita[56,48], L.A. Núñez[30], C. Oliveira[19], M. Palatka[32], J. Pallotta[9], S. Panja[32], G. Parente[79], T. Paulsen[38], J. Pawlowsky[38], M. Pech[32], J. Pękala[70], R. Pelayo[65], L.A.S. Pereira[23], E.E. Pereira Martins[39,7], J. Perez Armand[20], C. Pérez Bertolli[7,41], L. Perrone[56,48], S. Petrera[45,46], C. Petrucci[57,46], T. Pierog[41], M. Pimenta[72], M. Platino[7], B. Pont[80], M. Pothast[81,80], M. Pourmohammad Shahvar[61,47], P. Privitera[89], M. Prouza[32], A. Puyleart[87], S. Querchfeld[38], J. Rautenberg[38], D. Ravignani[7], M. Reininghaus[39], J. Ridky[32], F. Riehn[79], M. Risse[44], V. Rizi[57,46], W. Rodrigues de Carvalho[80], E. Rodriguez[7,41], J. Rodriguez Rojo[11], M.J. Roncoroni[7], S. Rossoni[43], M. Roth[41], E. Roulet[1], A.C. Rovero[4], P. Ruehl[44], A. Saftoiu[73], M. Saharan[80], F. Salamida[57,46], H. Salazar[64], G. Salina[51], J.D. Sanabria Gomez[30], F. Sánchez[7], E.M. Santos[20], E. Santos[32],

F. Sarazin[85], R. Sarmento[72], R. Sato[11], P. Savina[91], C.M. Schäfer[41], V. Scherini[56,48], H. Schieler[41], M. Schimassek[34], M. Schimp[38], F. Schlüter[41], D. Schmidt[39], O. Scholten[15,i], H. Schoorlemmer[80,81], P. Schovánek[32], F.G. Schröder[90,41], J. Schulte[42], T. Schulz[41], S.J. Sciutto[3], M. Scornavacche[7,41], A. Segreto[53,47], S. Sehgal[38], S.U. Shivashankara[76], G. Sigl[43], G. Silli[7], O. Sima[73,b], F. Simon[40], R. Smau[73], R. Šmída[89], P. Sommers[k], J.F. Soriano[86], R. Squartini[10], M. Stadelmaier[32], D. Stanca[73], S. Stanič[76], J. Stasielak[70], P. Stassi[36], S. Strähnz[39], M. Straub[42], M. Suárez-Durán[14], T. Suomijärvi[37], A.D. Supanitsky[7], Z. Svozilikova[32], Z. Szadkowski[71], A. Tapia[29], C. Taricco[63,52], C. Timmermans[81,80], O. Tkachenko[41], P. Tobiska[32], C.J. Todero Peixoto[18], B. Tomé[72], Z. Torrès[36], A. Travaini[10], P. Travnicek[32], C. Trimarelli[57,46], M. Tueros[3], M. Unger[41], L. Vaclavek[33], M. Vacula[33], J.F. Valdés Galicia[68], L. Valore[60,50], E. Varela[64], A. Vásquez-Ramírez[30], D. Veberič[41], C. Ventura[27], I.D. Vergara Quispe[3], V. Verzi[51], J. Vicha[32], J. Vink[83], J. Vlastimil[32], S. Vorobiov[76], C. Watanabe[26], A.A. Watson[c], A. Weindl[41], L. Wiencke[85], H. Wilczyński[70], D. Wittkowski[38], B. Wundheiler[7], B. Yue[38], A. Yushkov[32], O. Zapparrata[14], E. Zas[79], D. Zavrtanik[76,77], M. Zavrtanik[77,76]

[1] Centro Atómico Bariloche and Instituto Balseiro (CNEA-UNCuyo-CONICET), San Carlos de Bariloche, Argentina
[2] Departamento de Física and Departamento de Ciencias de la Atmósfera y los Océanos, FCEyN, Universidad de Buenos Aires and CONICET, Buenos Aires, Argentina
[3] IFLP, Universidad Nacional de La Plata and CONICET, La Plata, Argentina
[4] Instituto de Astronomía y Física del Espacio (IAFE, CONICET-UBA), Buenos Aires, Argentina
[5] Instituto de Física de Rosario (IFIR) – CONICET/U.N.R. and Facultad de Ciencias Bioquímicas y Farmacéuticas U.N.R., Rosario, Argentina
[6] Instituto de Tecnologías en Detección y Astropartículas (CNEA, CONICET, UNSAM), and Universidad Tecnológica Nacional – Facultad Regional Mendoza (CONICET/CNEA), Mendoza, Argentina
[7] Instituto de Tecnologías en Detección y Astropartículas (CNEA, CONICET, UNSAM), Buenos Aires, Argentina
[8] International Center of Advanced Studies and Instituto de Ciencias Físicas, ECyT-UNSAM and CONICET, Campus Miguelete – San Martín, Buenos Aires, Argentina
[9] Laboratorio Atmósfera – Departamento de Investigaciones en Láseres y sus Aplicaciones – UNIDEF (CITEDEF-CONICET), Argentina
[10] Observatorio Pierre Auger, Malargüe, Argentina
[11] Observatorio Pierre Auger and Comisión Nacional de Energía Atómica, Malargüe, Argentina
[12] Universidad Tecnológica Nacional – Facultad Regional Buenos Aires, Buenos Aires, Argentina
[13] University of Adelaide, Adelaide, S.A., Australia
[14] Université Libre de Bruxelles (ULB), Brussels, Belgium
[15] Vrije Universiteit Brussels, Brussels, Belgium
[16] Centro Federal de Educação Tecnológica Celso Suckow da Fonseca, Petropolis, Brazil
[17] Instituto Federal de Educação, Ciência e Tecnologia do Rio de Janeiro (IFRJ), Brazil
[18] Universidade de São Paulo, Escola de Engenharia de Lorena, Lorena, SP, Brazil
[19] Universidade de São Paulo, Instituto de Física de São Carlos, São Carlos, SP, Brazil
[20] Universidade de São Paulo, Instituto de Física, São Paulo, SP, Brazil
[21] Universidade Estadual de Campinas, IFGW, Campinas, SP, Brazil
[22] Universidade Estadual de Feira de Santana, Feira de Santana, Brazil
[23] Universidade Federal de Campina Grande, Centro de Ciencias e Tecnologia, Campina Grande, Brazil
[24] Universidade Federal do ABC, Santo André, SP, Brazil
[25] Universidade Federal do Paraná, Setor Palotina, Palotina, Brazil
[26] Universidade Federal do Rio de Janeiro, Instituto de Física, Rio de Janeiro, RJ, Brazil
[27] Universidade Federal do Rio de Janeiro (UFRJ), Observatório do Valongo, Rio de Janeiro, RJ, Brazil
[28] Universidade Federal Fluminense, EEIMVR, Volta Redonda, RJ, Brazil
[29] Universidad de Medellín, Medellín, Colombia
[30] Universidad Industrial de Santander, Bucaramanga, Colombia



PoS(ICRC2023)439

[31] Charles University, Faculty of Mathematics and Physics, Institute of Particle and Nuclear Physics, Prague, Czech Republic
[32] Institute of Physics of the Czech Academy of Sciences, Prague, Czech Republic
[33] Palacky University, Olomouc, Czech Republic
[34] CNRS/IN2P3, IJCLab, Université Paris-Saclay, Orsay, France
[35] Laboratoire de Physique Nucléaire et de Hautes Energies (LPNHE), Sorbonne Université, Université de Paris, CNRS-IN2P3, Paris, France
[36] Univ. Grenoble Alpes, CNRS, Grenoble Institute of Engineering Univ. Grenoble Alpes, LPSC-IN2P3, 38000 Grenoble, France
[37] Université Paris-Saclay, CNRS/IN2P3, IJCLab, Orsay, France
[38] Bergische Universität Wuppertal, Department of Physics, Wuppertal, Germany
[39] Karlsruhe Institute of Technology (KIT), Institute for Experimental Particle Physics, Karlsruhe, Germany
[40] Karlsruhe Institute of Technology (KIT), Institut für Prozessdatenverarbeitung und Elektronik, Karlsruhe, Germany
[41] Karlsruhe Institute of Technology (KIT), Institute for Astroparticle Physics, Karlsruhe, Germany
[42] RWTH Aachen University, III. Physikalisches Institut A, Aachen, Germany
[43] Universität Hamburg, II. Institut für Theoretische Physik, Hamburg, Germany
[44] Universität Siegen, Department Physik – Experimentelle Teilchenphysik, Siegen, Germany
[45] Gran Sasso Science Institute, L'Aquila, Italy
[46] INFN Laboratori Nazionali del Gran Sasso, Assergi (L'Aquila), Italy
[47] INFN, Sezione di Catania, Catania, Italy
[48] INFN, Sezione di Lecce, Lecce, Italy
[49] INFN, Sezione di Milano, Milano, Italy
[50] INFN, Sezione di Napoli, Napoli, Italy
[51] INFN, Sezione di Roma "Tor Vergata", Roma, Italy
[52] INFN, Sezione di Torino, Torino, Italy
[53] Istituto di Astrofisica Spaziale e Fisica Cosmica di Palermo (INAF), Palermo, Italy
[54] Osservatorio Astrofisico di Torino (INAF), Torino, Italy
[55] Politecnico di Milano, Dipartimento di Scienze e Tecnologie Aerospaziali , Milano, Italy
[56] Università del Salento, Dipartimento di Matematica e Fisica "E. De Giorgi", Lecce, Italy
[57] Università dell'Aquila, Dipartimento di Scienze Fisiche e Chimiche, L'Aquila, Italy
[58] Università di Catania, Dipartimento di Fisica e Astronomia "Ettore Majorana", Catania, Italy
[59] Università di Milano, Dipartimento di Fisica, Milano, Italy
[60] Università di Napoli "Federico II", Dipartimento di Fisica "Ettore Pancini", Napoli, Italy
[61] Università di Palermo, Dipartimento di Fisica e Chimica "E. Segrè", Palermo, Italy
[62] Università di Roma "Tor Vergata", Dipartimento di Fisica, Roma, Italy
[63] Università Torino, Dipartimento di Fisica, Torino, Italy
[64] Benemérita Universidad Autónoma de Puebla, Puebla, México
[65] Unidad Profesional Interdisciplinaria en Ingeniería y Tecnologías Avanzadas del Instituto Politécnico Nacional (UPIITA-IPN), México, D.F., México
[66] Universidad Autónoma de Chiapas, Tuxtla Gutiérrez, Chiapas, México
[67] Universidad Michoacana de San Nicolás de Hidalgo, Morelia, Michoacán, México
[68] Universidad Nacional Autónoma de México, México, D.F., México
[69] Universidad Nacional de San Agustin de Arequipa, Facultad de Ciencias Naturales y Formales, Arequipa, Peru
[70] Institute of Nuclear Physics PAN, Krakow, Poland
[71] University of Łódź, Faculty of High-Energy Astrophysics,Łódź, Poland
[72] Laboratório de Instrumentação e Física Experimental de Partículas – LIP and Instituto Superior Técnico – IST, Universidade de Lisboa – UL, Lisboa, Portugal
[73] "Horia Hulubei" National Institute for Physics and Nuclear Engineering, Bucharest-Magurele, Romania
[74] Institute of Space Science, Bucharest-Magurele, Romania
[75] University Politehnica of Bucharest, Bucharest, Romania
[76] Center for Astrophysics and Cosmology (CAC), University of Nova Gorica, Nova Gorica, Slovenia
[77] Experimental Particle Physics Department, J. Stefan Institute, Ljubljana, Slovenia

PoS(ICRC2023)439

[78] Universidad de Granada and C.A.F.P.E., Granada, Spain
[79] Instituto Galego de Física de Altas Enerxías (IGFAE), Universidade de Santiago de Compostela, Santiago de Compostela, Spain
[80] IMAPP, Radboud University Nijmegen, Nijmegen, The Netherlands
[81] Nationaal Instituut voor Kernfysica en Hoge Energie Fysica (NIKHEF), Science Park, Amsterdam, The Netherlands
[82] Stichting Astronomisch Onderzoek in Nederland (ASTRON), Dwingeloo, The Netherlands
[83] Universiteit van Amsterdam, Faculty of Science, Amsterdam, The Netherlands
[84] Case Western Reserve University, Cleveland, OH, USA
[85] Colorado School of Mines, Golden, CO, USA
[86] Department of Physics and Astronomy, Lehman College, City University of New York, Bronx, NY, USA
[87] Michigan Technological University, Houghton, MI, USA
[88] New York University, New York, NY, USA
[89] University of Chicago, Enrico Fermi Institute, Chicago, IL, USA
[90] University of Delaware, Department of Physics and Astronomy, Bartol Research Institute, Newark, DE, USA
[91] University of Wisconsin-Madison, Department of Physics and WIPAC, Madison, WI, USA

—

[a] Louisiana State University, Baton Rouge, LA, USA
[b] also at University of Bucharest, Physics Department, Bucharest, Romania
[c] School of Physics and Astronomy, University of Leeds, Leeds, United Kingdom
[d] now at Agenzia Spaziale Italiana (ASI). Via del Politecnico 00133, Roma, Italy
[e] Fermi National Accelerator Laboratory, Fermilab, Batavia, IL, USA
[f] now at Graduate School of Science, Osaka Metropolitan University, Osaka, Japan
[g] now at ECAP, Erlangen, Germany
[h] Max-Planck-Institut für Radioastronomie, Bonn, Germany
[i] also at Kapteyn Institute, University of Groningen, Groningen, The Netherlands
[j] Colorado State University, Fort Collins, CO, USA
[k] Pennsylvania State University, University Park, PA, USA

## Acknowledgments

The successful installation, commissioning, and operation of the Pierre Auger Observatory would not have been possible without the strong commitment and effort from the technical and administrative staff in Malargüe. We are very grateful to the following agencies and organizations for financial support:

Argentina – Comisión Nacional de Energía Atómica; Agencia Nacional de Promoción Científica y Tecnológica (ANPCyT); Consejo Nacional de Investigaciones Científicas y Técnicas (CONICET); Gobierno de la Provincia de Mendoza; Municipalidad de Malargüe; NDM Holdings and Valle Las Leñas; in gratitude for their continuing cooperation over land access; Australia – the Australian Research Council; Belgium – Fonds de la Recherche Scientifique (FNRS); Research Foundation Flanders (FWO); Brazil – Conselho Nacional de Desenvolvimento Científico e Tecnológico (CNPq); Financiadora de Estudos e Projetos (FINEP); Fundação de Amparo à Pesquisa do Estado de Rio de Janeiro (FAPERJ); São Paulo Research Foundation (FAPESP) Grants No. 2019/10151-2, No. 2010/07359-6 and No. 1999/05404-3; Ministério da Ciência, Tecnologia, Inovações e Comunicações (MCTIC); Czech Republic – Grant No. MSMT CR LTT18004, LM2015038, LM2018102, CZ.02.1.01/0.0/0.0/16_013/0001402, CZ.02.1.01/0.0/0.0/18_046/0016010 and CZ.02.1.01/0.0/0.0/17_049/0008422; France – Centre de Calcul IN2P3/CNRS; Centre National de la Recherche Scientifique (CNRS); Conseil Régional Ile-de-France; Département Physique Nucléaire et Corpusculaire (PNC-IN2P3/CNRS); Département Sciences de l'Univers (SDU-INSU/CNRS); Institut Lagrange de Paris (ILP) Grant No. LABEX ANR-10-LABX-63 within the Investissements d'Avenir Programme Grant No. ANR-11-IDEX-0004-02; Germany – Bundesministerium für Bildung und Forschung (BMBF); Deutsche Forschungsgemeinschaft (DFG); Finanzministerium Baden-Württemberg; Helmholtz Alliance for Astroparticle Physics (HAP); Helmholtz-Gemeinschaft Deutscher Forschungszentren (HGF); Ministerium für Kultur und Wissenschaft des Landes Nordrhein-Westfalen; Ministerium für Wissenschaft, Forschung und Kunst des Landes Baden-Württemberg; Italy – Istituto Nazionale di Fisica Nucleare (INFN); Istituto Nazionale di Astrofisica (INAF); Ministero dell'Universitá e della Ricerca (MUR); CETEMPS Center of Excellence; Ministero degli Affari Esteri (MAE), ICSC Centro Nazionale di Ricerca in High Performance Computing, Big Data

and Quantum Computing, funded by European Union NextGenerationEU, reference code CN_00000013; México – Consejo Nacional de Ciencia y Tecnología (CONACYT) No. 167733; Universidad Nacional Autónoma de México (UNAM); PAPIIT DGAPA-UNAM; The Netherlands – Ministry of Education, Culture and Science; Netherlands Organisation for Scientific Research (NWO); Dutch national e-infrastructure with the support of SURF Cooperative; Poland – Ministry of Education and Science, grants No. DIR/WK/2018/11 and 2022/WK/12; National Science Centre, grants No. 2016/22/M/ST9/00198, 2016/23/B/ST9/01635, 2020/39/B/ST9/01398, and 2022/45/B/ST9/02163; Portugal – Portuguese national funds and FEDER funds within Programa Operacional Factores de Competitividade through Fundação para a Ciência e a Tecnologia (COMPETE); Romania – Ministry of Research, Innovation and Digitization, CNCS-UEFISCDI, contract no. 30N/2023 under Romanian National Core Program LAPLAS VII, grant no. PN 23 21 01 02 and project number PN-III-P1-1.1-TE-2021-0924/TE57/2022, within PNCDI III; Slovenia – Slovenian Research Agency, grants P1-0031, P1-0385, I0-0033, N1-0111; Spain – Ministerio de Economía, Industria y Competitividad (FPA2017-85114-P and PID2019-104676GB-C32), Xunta de Galicia (ED431C 2017/07), Junta de Andalucía (SOMM17/6104/UGR, P18-FR-4314) Feder Funds, RENATA Red Nacional Temática de Astropartículas (FPA2015-68783-REDT) and María de Maeztu Unit of Excellence (MDM-2016-0692); USA – Department of Energy, Contracts No. DE-AC02-07CH11359, No. DE-FR02-04ER41300, No. DE-FG02-99ER41107 and No. DE-SC0011689; National Science Foundation, Grant No. 0450696; The Grainger Foundation; Marie Curie-IRSES/EPLANET; European Particle Physics Latin American Network; and UNESCO.